

**[*n*]Pseudorotaxanes constructed by a bis(*p*-phenylene)-
34-crown-10-based cryptand: different binding behaviors
induced by minor structural changes of guests**

Haoze Wang, Peifa Wei,* and Xuzhou Yan*

Department of Chemistry, Zhejiang University, Hangzhou 310027, P. R. China

Email: pfwei@zju.edu.cn, xzyan@zju.edu.cn

Electronic Supplementary Information (14 pages)

1. <i>Materials and methods</i>	S2
2. <i>Partial ¹H NMR spectrum of host 1</i>	S3
3. <i>Job plots of 1⇌2, 1⇌3, and 1⇌4 based on UV-vis in acetone</i>	S4
4. <i>LRESIMS of host 1 with guests 2, 3, and 4 in acetone</i>	S7
5. <i>Association constants of 1⇌2, 1⇌3, and 1⇌4 in acetone</i>	S9
6. <i>X-ray analysis data for 1⇌2, 1₂⇌3, and 1⇌4</i>	S13
<i>References</i>	S14

1. *Materials and methods*

Bis(*p*-phenylene)-34-crown-10 (BPP34C10)-based cryptand^{S1} was synthesized

according to a literature procedure. All reagents were commercially available and used as supplied without further purification. Solvents were either employed as purchased or dried according to procedures described in the literature. NMR spectra were recorded with a Bruker Advance DMX 500 spectrophotometer or a Bruker Advance DMX 400 spectrophotometer with the deuterated solvent as the lock and the residual solvent or TMS as the internal reference. ^1H and ^{13}C NMR chemical shifts are reported relative to residual solvent signals. Mass spectra were recorded on a Micromass Quattro II triple-quadrupole mass spectrometer using electrospray ionization with a MassLynx operating system or a Bruker Esquire 3000 plus mass spectrometer (Bruker-Franzen Analytik GmbH, Bremen, Germany) equipped with an ESI interface and an ion trap analyzer. UV-vis spectroscopy was performed on a Shimadzu UV-2550 instrument at room temperature. The crystal data were collected on an Oxford Diffraction Xcalibur Atlas Gemini ultra instrument. The crystal structures were solved by SHELXS-97^{S2} and refined by SHELXL-97.^{S3}

2. Partial ^1H NMR spectra of host 1

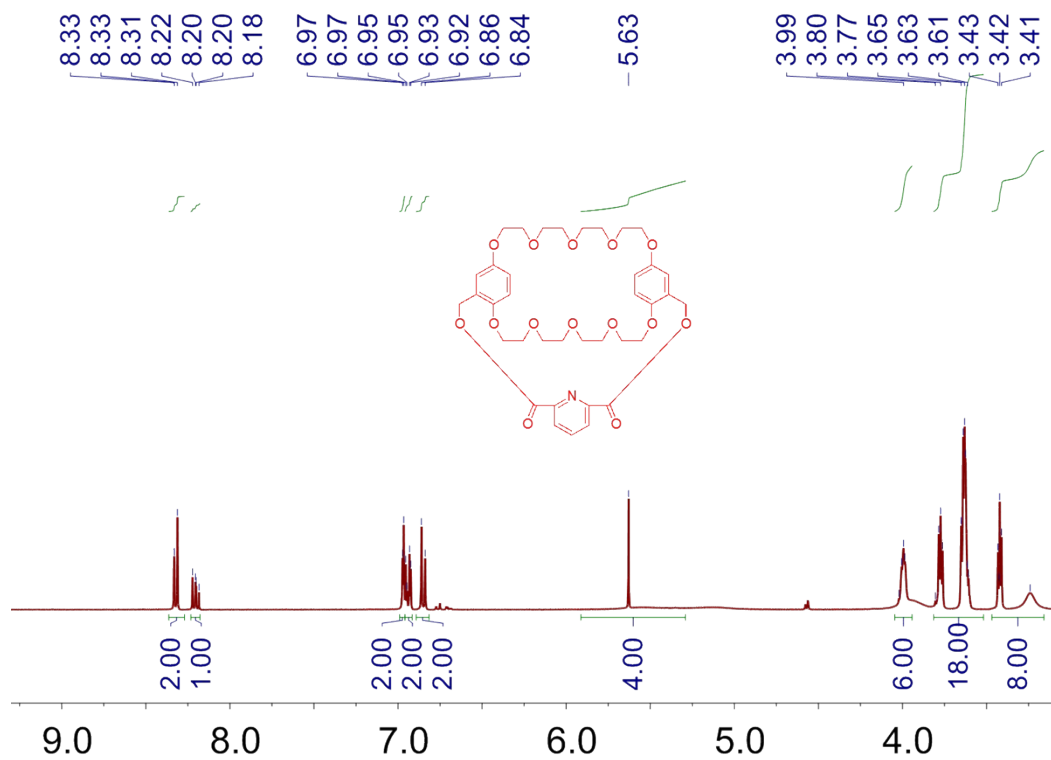


Figure S1. ¹H NMR spectrum (acetone-*d*₆, 293 K, 400 MHz) of **1**.

3. Job plots of **1**→**2**, **1**→**3**, and **1**→**4** based on UV-vis in acetone

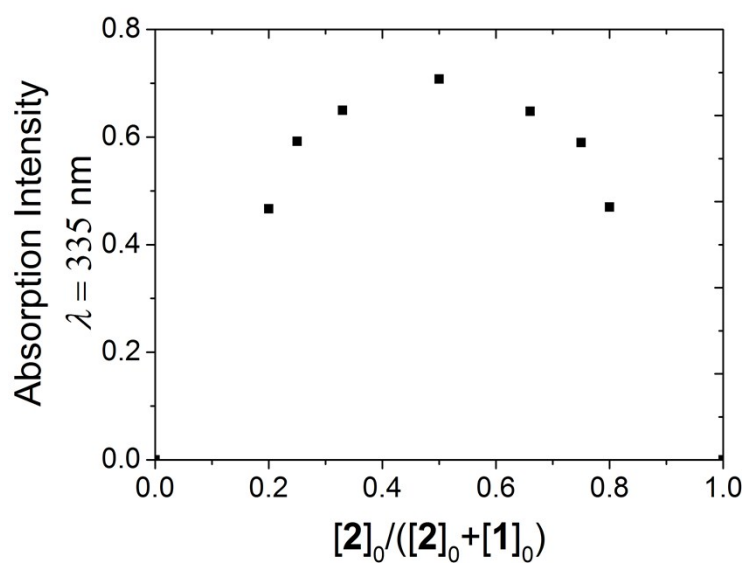
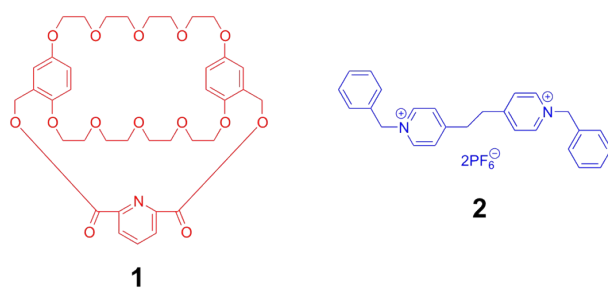


Figure S2. Job plot showing the 1:1 stoichiometry of the complexation between **1** and **2** in acetone: $[1]_0 + [2]_0 = 1.00 \text{ mM}$; $[1]_0$ and $[2]_0$ are the initial concentrations of **1** and **2**.

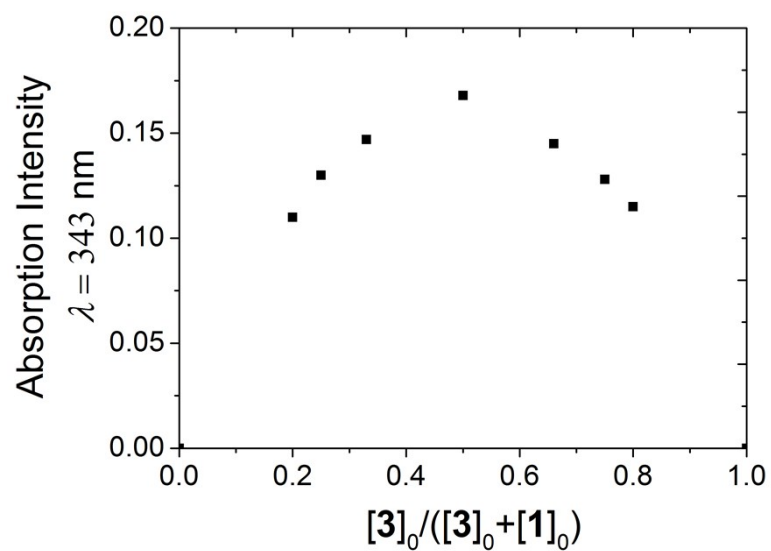
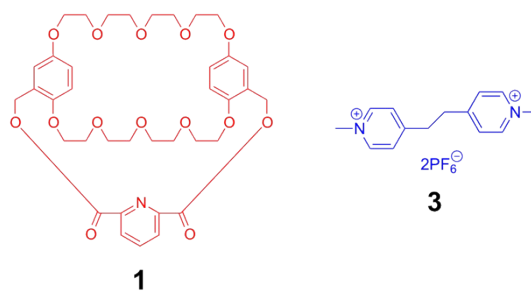


Figure S3. Job plot showing the 1:1 stoichiometry of the complexation between **1** and **3** in acetone: $[1]_0 + [3]_0 = 1.00 \text{ mM}$; $[1]_0$ and $[3]_0$ are the initial concentrations of **1** and **3**.

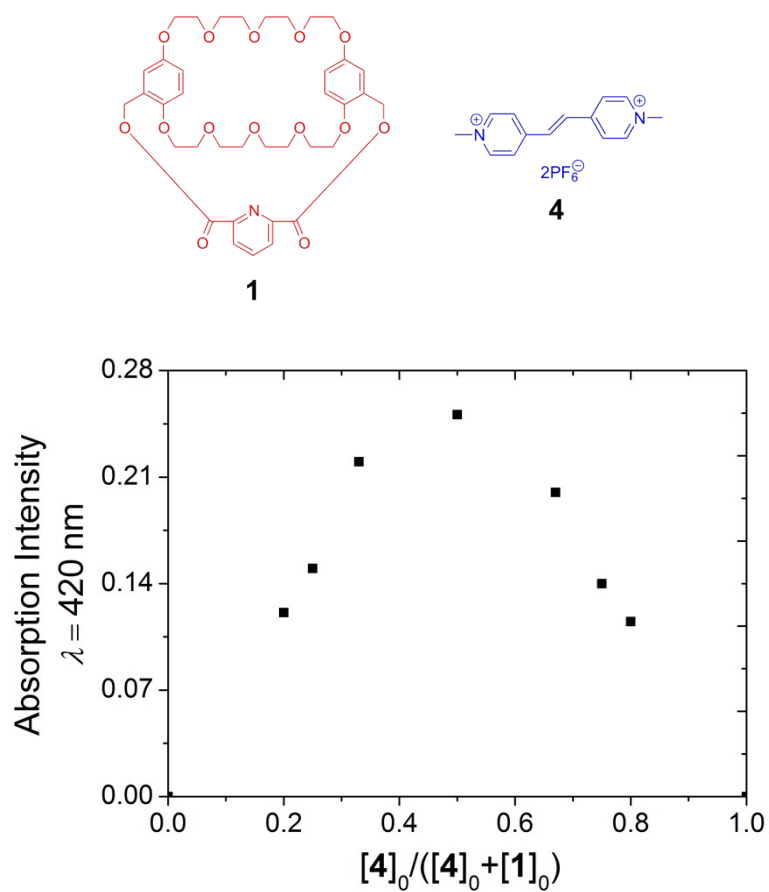


Figure S4. Job plot showing the 1:1 stoichiometry of the complexation between **1** and **4** in acetone: $[1]_0 + [4]_0 = 1.00$ mM; $[1]_0$ and $[4]_0$ are the initial concentrations of **1** and **4**.

4. LRESIMS of host **1** with guests **2**, **3**, and **4** in acetone

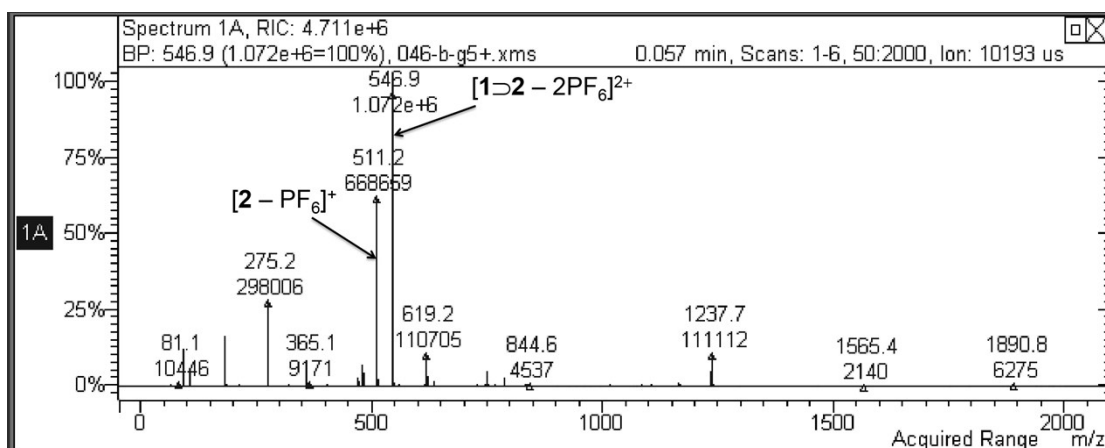


Figure S5. The positive electrospray ionization mass spectrum of an equimolar mixture of **1** and **2** in acetone. Mass fragment at m/z 546.9 for $[1 \rightarrow 2 - 2PF_6]^{2+}$ confirmed the 1:1 complexation stoichiometry between **1** and **2**.

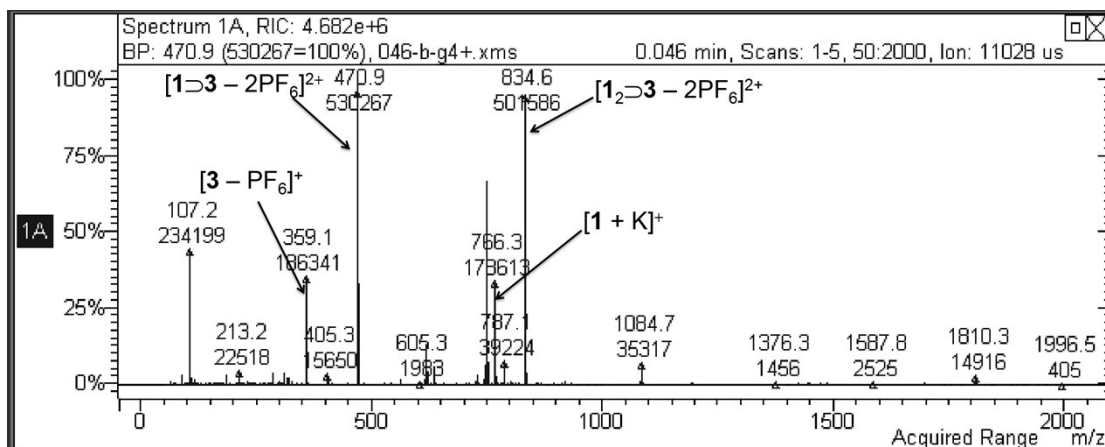


Figure S6. The positive electrospray ionization mass spectrum of an equimolar mixture of **1** and **3** in acetone. Mass fragments at m/z 470.9 for $[1 \rightarrow 3 - 2PF_6]^{2+}$ and m/z 834.6 for $[1_2 \rightarrow 3 - 2PF_6]^{2+}$ indicated the possible 1:1 and 2:1 complexation stoichiometries between **1** and **3** in gaseous phase.

Display Report

Analysis Info		Acquisition Date	05/19/14 20:16:14
Analysis Name	14051926.d	Operator	Administrator
Method	Copy of E3Kp Default.ms	Instrument	esquire3000plus
Sample Name	IjY-046B-G10		
Comment			

Acquisition Parameter			
Ion Source Type	ESI	Ion Polarity	Positive
Mass Range Mode	Std/Normal	Scan Begin	50 m/z
Capillary Exit	181.0 Volt	Skim 1	40.0 Volt
Accumulation Time	401 μ s	Averages	5 Spectra
		Alternating Ion Polarity	off
		Scan End	2000 m/z
		Trap Drive	135.4
		Auto MS/MS	off

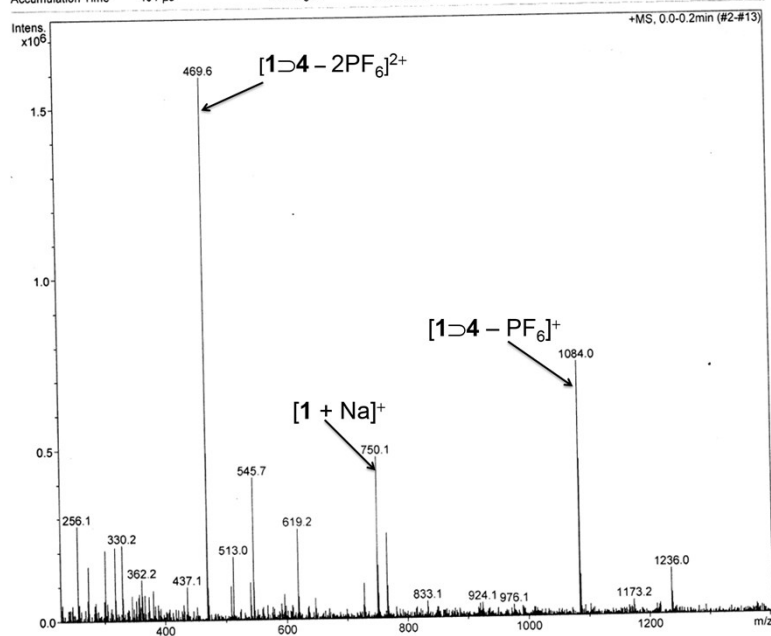


Figure S7. The positive electrospray ionization mass spectrum of an equimolar mixture of **1** and **4** in acetone. Mass fragments at m/z 469.6 for $[1>4 - 2PF_6]^{2+}$ and m/z 1084.0 for $[1>4 - PF_6]^+$ confirmed the 1:1 complexation stoichiometry between **1** and **4**.

5. Association constants of **1**→**2**, **1**→**3**, and **1**→**4** in acetone

The association constants (K_a) of complexes **1**→**2**, **1**→**3**, and **1**→**4** were determined by probing the charge-transfer bands of the complexes by UV-vis spectroscopy and employing a titration method. Progressive addition of an acetone solution with high guest concentration and low host concentration to an acetone solution with the same host concentration resulted in an increase of the intensity of the charge-transfer bands of the complexes. Treatment of the collected absorbance data with a non-linear curve-fitting program afforded the corresponding association constants (K_a): $4.65 (\pm 0.22) \times 10^2 \text{ M}^{-1}$ for **1**→**2**, $1.69 (\pm 0.23) \times 10^3 \text{ M}^{-1}$ for **1**→**3**, and $2.16 (\pm 0.21) \times 10^5 \text{ M}^{-1}$ for **1**→**4**, respectively. The non-linear curve-fitting was based on the equation:

$$A = (A_\infty/[H]_0) (0.5[G]_0 + 0.5([H]_0 + 1/K_a) - 0.5 ([G]_0^2 + 2[G]_0(1/K_a - [H]_0) + (1/K_a + [H]_0)^2)^{0.5})$$

(Eq. S1)

Wherein A is the absorption intensity of the charge-transfer band at $[G]_0$, A_∞ is the absorption intensity of the charge-transfer band when the host is completely complexed, $[H]_0$ is the fixed initial concentration of the host, and $[G]_0$ is the initial concentration of the guest.

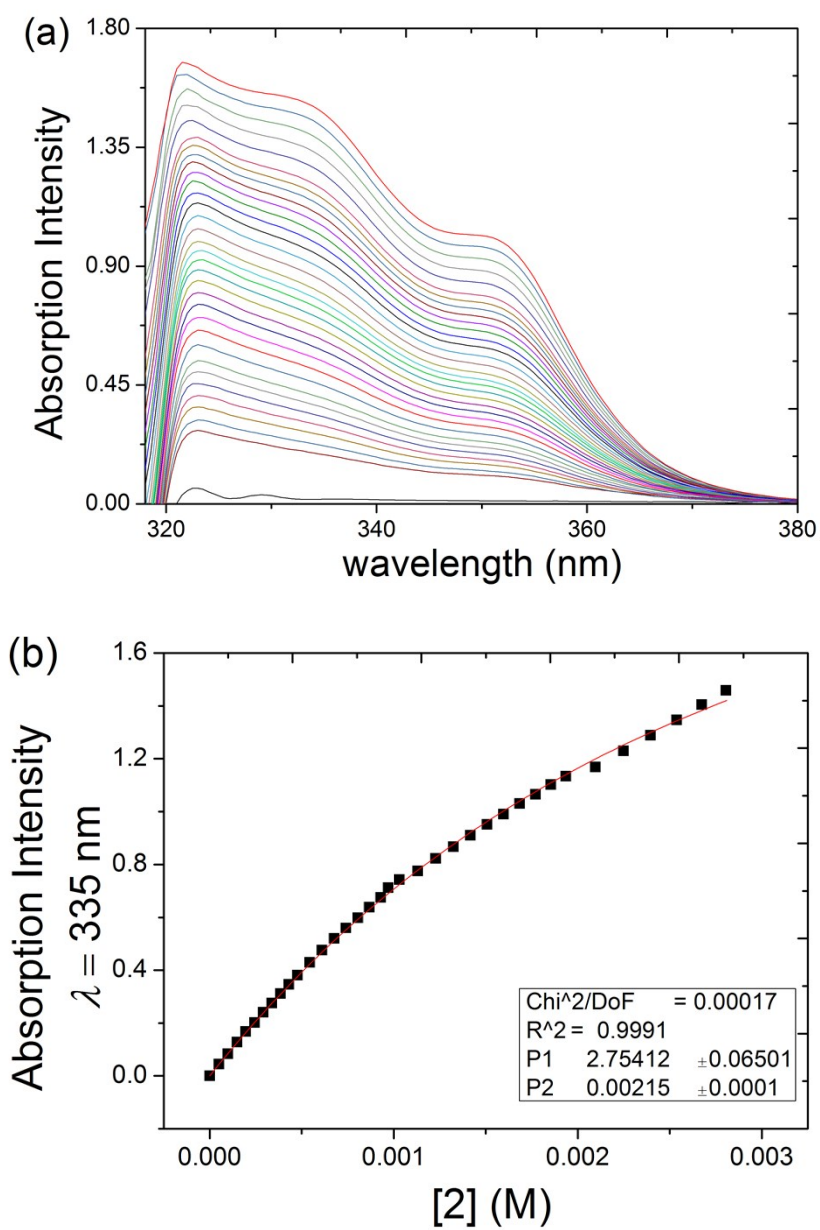
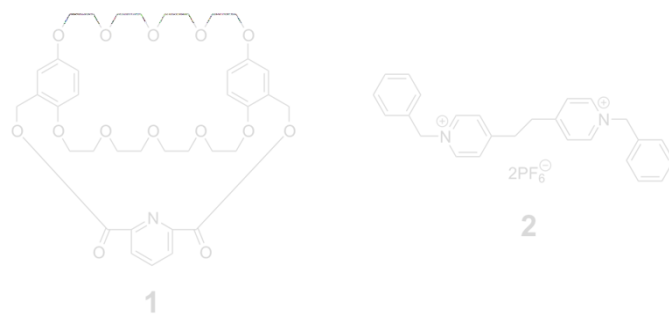


Figure S8. (a) The absorption spectral changes of **1** (1.00 mM) upon addition of **2** and (b) the absorption intensity changes at $\lambda = 335$ nm upon addition of **2** (from 0 to 2.81 mM). The red solid line was obtained from the non-linear curve-fitting using Eq. S1.

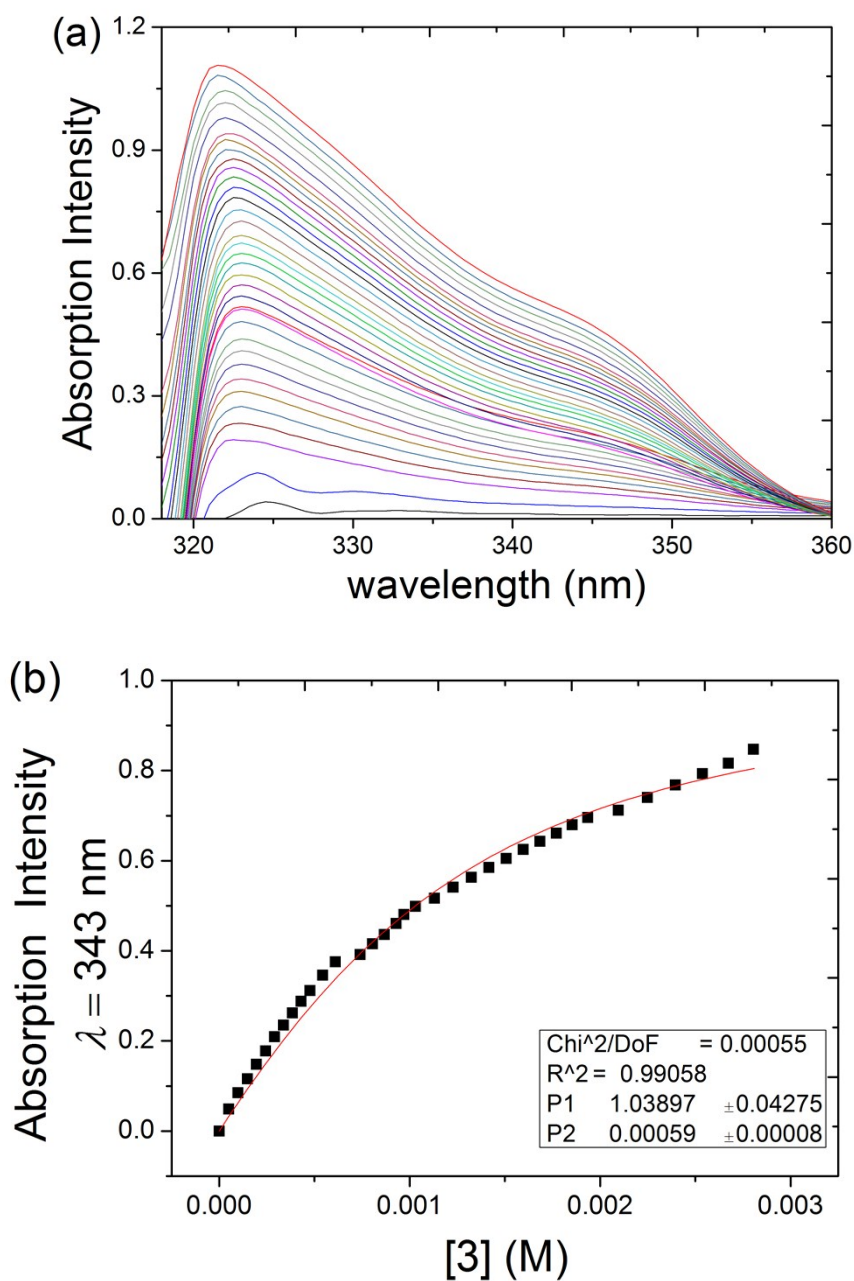
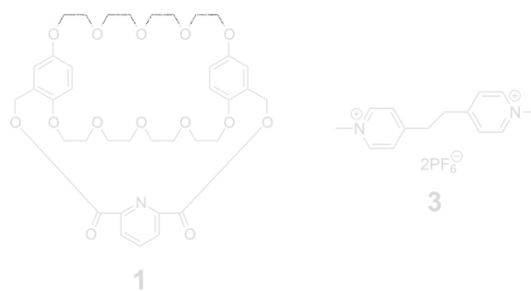


Figure S9. (a) The absorption spectral changes of **1** (1.00 mM) upon addition of **3** and (b) the absorption intensity changes at $\lambda = 343 \text{ nm}$ upon addition of **3** (from 0 to 2.81 mM). The red solid line was obtained from the non-linear curve-fitting using Eq. S1.

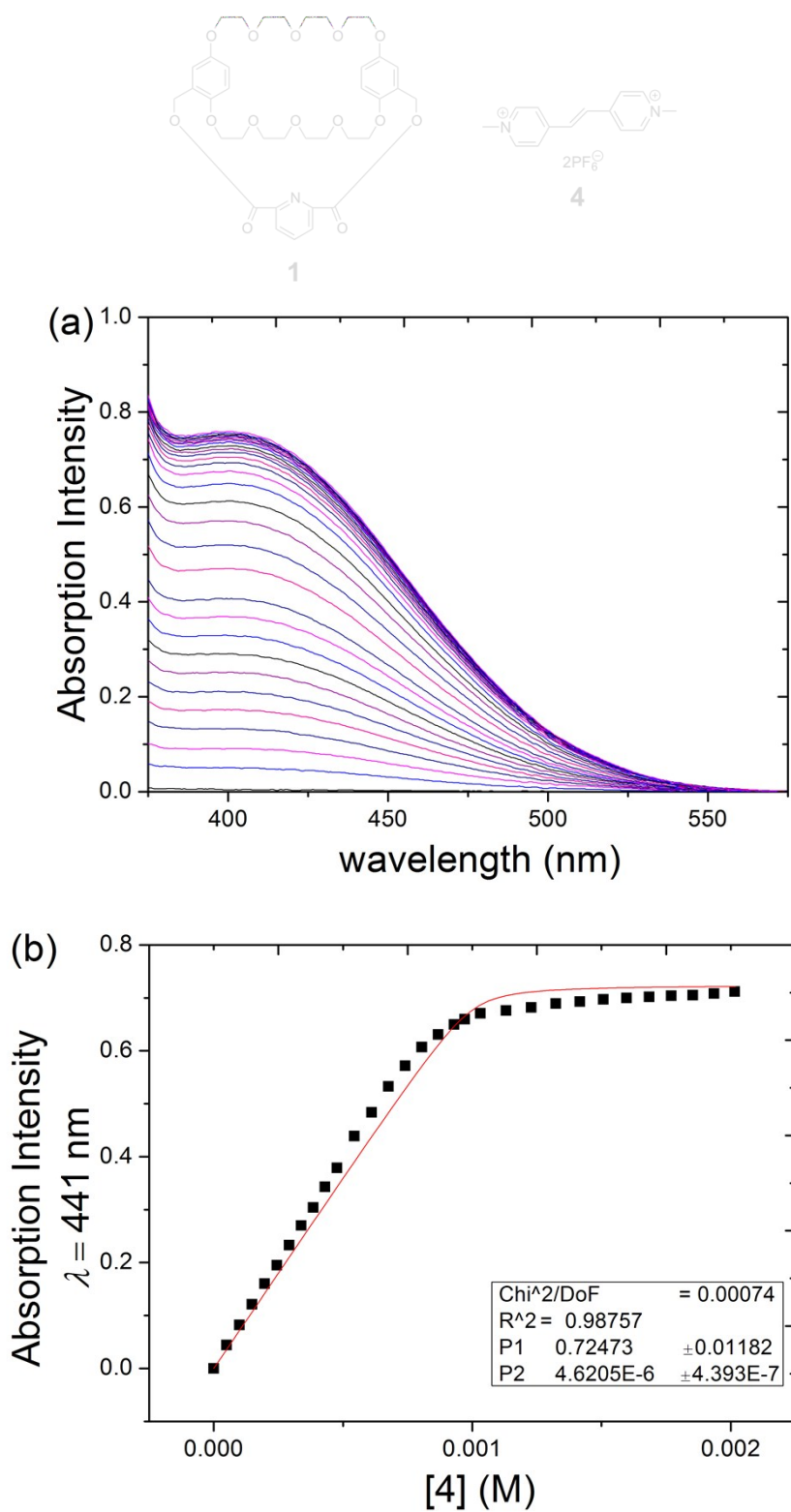


Figure S10. (a) The absorption spectral changes of **1** (1.00 mM) upon addition of **4** and (b) the absorption intensity changes at $\lambda = 441$ nm upon addition of **4** (from 0 to 2.02 mM). The red solid line was obtained from the non-linear curve-fitting using Eq. S1.

6. X-ray analysis data for **1**→**2**, **1**→**3**, and **1**→**4**

Crystallographic data for **1**→**2**: block, yellow, $0.38 \times 0.29 \times 0.2 \text{ mm}^3$, $\text{C}_{67}\text{H}_{76}\text{F}_{12}\text{N}_5\text{O}_{14}\text{P}_2$, *FW* 1465.27, triclinic, space group $P \bar{1}$, $a = 16.4730(6)$, $b = 21.0698(6)$, $c = 22.2668(7) \text{ \AA}$, $\alpha = 101.201(3)^\circ$, $\beta = 99.999(3)^\circ$, $\gamma = 108.199(3)^\circ$, $V = 6970.6(4) \text{ \AA}^3$, $Z = 4$, $D_c = 1.396 \text{ g cm}^{-3}$, $T = 170 \text{ K}$, $\mu = 0.161 \text{ mm}^{-1}$, 15140 measured reflections, 25454 independent reflections, 1805 parameters, 0 restraints, $F(000) = 3052.0$, $R_1 = 0.1390$, $wR_1 = 0.0883$ (all data), $R_2 = 0.2979$, $wR_2 = 0.2476$ [$I > 2\sigma(I)$], max. residual density $1.332 \text{ e}\cdot\text{\AA}^{-3}$, and goodness-of-fit (F^2) = 1.038. CCDC 1046153.

Crystallographic data for **1**→**3**: platelet, yellow, $0.32 \times 0.3 \times 0.23 \text{ mm}^3$, $\text{C}_{46}\text{H}_{59}\text{F}_6\text{N}_3\text{O}_{15}\text{P}$, *FW* 1038.93, triclinic, space group $P \bar{1}$, $a = 10.9381(5)$, $b = 11.7474(7)$, $c = 19.8477(9) \text{ \AA}$, $\alpha = 101.306(4)^\circ$, $\beta = 99.715(4)^\circ$, $\gamma = 94.513(4)^\circ$, $V = 2448.4(2) \text{ \AA}^3$, $Z = 2$, $D_c = 1.409 \text{ g cm}^{-3}$, $T = 170 \text{ K}$, $\mu = 0.150 \text{ mm}^{-1}$, 5447 measured reflections, 8937 independent reflections, 677 parameters, 2 restraints, $F(000) = 1090.0$, $R_1 = 0.1174$, $wR_1 = 0.0726$ (all data), $R_2 = 0.2234$, $wR_2 = 0.1816$ [$I > 2\sigma(I)$], max. residual density $0.802 \text{ e}\cdot\text{\AA}^{-3}$, and goodness-of-fit (F^2) = 1.146. CCDC 1046154.

Crystallographic data for **1**→**4**: platelet, yellow, $0.45 \times 0.35 \times 0.2 \text{ mm}^3$, $\text{C}_{53}\text{H}_{64}\text{F}_{12}\text{N}_4\text{O}_{14}\text{P}_2$, *FW* 1271.02, monoclinic, space group $C 1 2/c 1$, $a = 54.999(2)$, $b = 11.2922(4)$, $c = 19.9536(9) \text{ \AA}$, $\alpha = 90.00^\circ$, $\beta = 98.733(4)^\circ$, $\gamma = 90.00^\circ$, $V = 12248.8(9) \text{ \AA}^3$, $Z = 8$, $D_c = 1.378 \text{ g cm}^{-3}$, $T = 170 \text{ K}$, $\mu = 0.171 \text{ mm}^{-1}$, 8007 measured reflections, 11014 independent reflections, 832 parameters, 0 restraints, $F(000) = 5280.0$, $R_1 = 0.1116$, $wR_1 = 0.0884$ (all data), $R_2 = 0.2919$, $wR_2 = 0.2631$ [$I > 2\sigma(I)$], max. residual density $1.438 \text{ e}\cdot\text{\AA}^{-3}$, and goodness-of-fit (F^2) = 1.047. CCDC 1046155.

References:

- S1. P. Wei, Z. Li and B. Xia, *Tetrahedron Letters*, 2014, **55**, 5825–5828.
- S2. G. M. Sheldrick, *SHELXS-97, Program for solution of crystal structures*, University of Göttingen, Germany, 1990.
- S3. G. M. Sheldrick, *SHELXS-97, Program for refinement of crystal structures*, University of Göttingen, Germany, 1997.